Received: 25 April 2024 | Revised: 13 June 2024 | Accepted: 29 June 2024

DOI: 10.1002/arch.22133

RESEARCH ARTICLE

Archives of INSECT BIOCHEMISTRY AND PHYSIOLOGY WILEY

Composition and abundance of midgut plasma membrane proteins in two major hemipteran vectors of plant viruses, *Bemisia tabaci* and *Myzus persicae*

Jaime Jiménez | **Ruchir Mishra** | **Xinyue Wang** | **Ciara M. Magee** | **Bryony C. Bonning**

Department of Entomology and Nematology, University of Florida, Gainesville, Florida, USA

Correspondence
Bryony C. Bonning, Department of Entomology & Nematology, University of Florida, PO Box 110620, Gainesville, FL 32611-0620, USA.
Email: bbonning@ufl.edu

Present address
Jaime Jiménez, Instituto de Ciencias Agrarias – Consejo Superior de Investigaciones Científicas (ICA-CSIC), Madrid, Spain.

Funding information
National Science Foundation, Grant/Award Numbers: 2310815, IIP-1821914

Abstract

Multiple species within the order Hemiptera cause severe agricultural losses on a global scale. Aphids and whiteflies are of particular importance due to their role as vectors for hundreds of plant viruses, many of which enter the insect via the gut. To facilitate the identification of novel targets for disruption of plant virus transmission, we compared the relative abundance and composition of the gut plasma membrane proteomes of adult *Bemisia tabaci* (Hemiptera: Aleyrodidae) and *Myzus persicae* (Hemiptera: Aphididae), representing the first study comparing the gut plasma membrane proteomes of two different insect species. Brush border membrane vesicles were prepared from dissected guts, and proteins extracted, identified and quantified from triplicate samples via timsTOF mass spectrometry. A total of 1699 *B. tabaci* and 1175 *M. persicae* proteins were identified. Following bioinformatics analysis and manual curation, 151 *B. tabaci* and 115 *M. persicae* proteins were predicted to localize to the plasma membrane of the gut microvilli. These proteins were further categorized based on molecular function and biological process according to Gene Ontology terms. The most

abundant gut plasma membrane proteins were identified. The ten plasma membrane proteins that differed in abundance between the two insect species were associated with the terms "protein binding" and "viral processes." In addition to providing insight into the gut physiology of hemipteran insects, these gut plasma membrane proteomes provide context for appropriate identification of plant virus receptors based on a combination of bioinformatic prediction and protein localization on the surface of the insect gut.

KEYWORDS

gut receptors, Hemiptera, insect gut, plant virus, proteome, whitefly

Key points

- The most abundant *Bemisia tabaci* and *Myzus persicae* gut plasma membrane and gut surface proteins were identified.
- This work informs appropriate localization to the gut surface of candidate receptor proteins for plant viruses vectored by these insects.
- In silico prediction of likely plant virus receptors based on machine learning-enhanced bioinformatic tools are discussed.

1 | INTRODUCTION

Hemipteran insects that feed on phloem are responsible for the transmission of many plant pathogens. Indeed, the majority of plant viruses are transmitted by hemipteran insects with more than half transmitted by whiteflies or aphids (Fereres & Raccah, 2015; Hogenhout et al., 2008). Primary vectors among these are the sweet potato whitefly, *Bemisia tabaci* (Hemiptera: Aleyrodidae) (Ghosh & Ghanim, 2021), and the green peach aphid, *Myzus persicae* (Ng & Perry, 2004). *B. tabaci* transmits more than 400 plant viruses (Ghosh & Ghanim, 2021) with begomoviruses (*Geminiviridae*) being the largest group of viruses transmitted specifically by whiteflies. Begomoviruses cause 20%–100% reduction in vegetable crop yield (Polston & Anderson, 1997) with annual losses of more than US $300 million (Navas-Castillo et al., 2011; Varma & Malathi, 2003). *M. persicae* vectors more than 100 persistent plant viruses (Blackman & Eastop, 2000) of which luteoviruses (*Luteoviridae*) and poleroviruses (*Solemoviridae*), are of particular economic importance (Ng & Perry, 2004).

Many of these plant viruses are transmitted by their aphid and whitefly vectors in a circulative, non-propagative manner. In contrast to non-circulative viruses, which are retained in the stylets or foregut of their insect vectors, circulative viruses need to bind and cross the gut epithelium to be successfully acquired and transmitted by the vector (Ng & Perry, 2004). Following ingestion from the phloem of an infected plant, virions enter the gut lumen, bind to receptors on the surface of the insect gut epithelium, transcytose across the epithelium and enter the hemocoel. Some of the plant viruses circulating within the hemocoel bind to receptors on the salivary gland and

cross the salivary gland epithelium for release with the saliva during subsequent feeding (Czosnek et al., 2017; Gray & Gildow, 2003). The initial interaction of these circulative, non-propagative plant viruses with the insect vector is mediated by virus binding to specific proteins on the surface of the gut epithelium that mediate entry into the vector. As this initial virus-receptor association is a primary target for intervention to block virus transmission, the identity of plant virus receptors in the gut of the insect vector is of particular importance (Bonning, 2025).

The insect midgut epithelium includes at least four different cell types (Caccia et al., 2019), of which the columnar cells or enterocytes, are the most abundant. These cells have microvilli on their luminal surface that create a "brush border" with the large surface area facilitating nutrient absorption (Holtof et al., 2019). The proteins, glycans and lipids on the surface of the microvilli mediate virus binding and entry into the gut epithelial cells. Membrane proteins such as those on the microvillar membrane are divided into eight classes: single-pass membrane proteins, which have a single transmembrane helix (four classes), multipass transmembrane proteins, GPI-anchored, lipid-anchored proteins, and peripheral membrane proteins (Butt et al., 2017). Brush border membrane vesicles (BBMV), which are enriched in microvillar surface proteins, are useful for analysis of the insect gut surface proteome and for identification of virus receptors (Wolfersberger, 1993)

Relatively few studies have characterized the gut surface proteome in insects, with analyses of the *Trichoplusia ni* BBMV proteome (Javed et al., 2019) and *Aedes aegypti* lipid raft proteome (Bayyareddy et al., 2012) being notable exceptions. A more sensitive, quantitative proteomics method was used to compare the gut surface proteomes of adult and nymph *Diaphorina citri* (Tavares et al., 2022). Recently, enhanced bioinformatic tools were developed using machine learning for in silico prediction of viral receptor proteins. Using a generalized boosted model, Valero-Rello et al. (2024) explored plasma membrane protein features that predict whether a protein functions as a virus receptor with reference to 175 known mammalian receptor proteins (Valero-Rello et al., 2024). Using optimized parameters, this model correctly predicted > 90% of known receptors. The top four features for prediction of virus receptor function were the number of protein interactors, and the gene ontology (GO) terms "protein binding" (GO:0005515), "cell adhesion" (GO:0007155), and "cell surface" (GO:0009986). Among terms frequently used for classification based on high coverage that were not among the most decisive features in the analysis, were glycosylation, and immunoglobulin domain (Valero-Rello et al., 2024). Taken together, the reduced amount of material required for proteomic studies resulting from increasingly sensitive spectrometers (Meier et al., 2015, 2018), combined with improvements in protein identification technology and enhanced bioinformatic tools provide an unprecedented opportunity to identify the gut epithelial proteins of very small hemipteran species such as whiteflies and aphids.

The goal for this study was to identify the most abundant proteins in the plasma membrane of the midgut of *B. tabaci* and *M. persicae*, to (1) provide foundational information on hemipteran gut physiology, and (2) inform appropriate localization of candidate plant virus receptor proteins in these insect vectors for proteins predicted to localize to the gut surface. While several candidate receptor proteins have been identified in *B. tabaci* (cubulin, aminopeptidase N for the begomovirus, *Tomato yellow leaf curl virus*; TYLCV) (Fan et al., 2024; Zhao et al., 2020) and in *M. persicae* (ephrin for the luteovirus, *Turnip yellows virus*) (Mulot et al., 2018), localization of these proteins to the gut surface has not been confirmed. To this end, we performed proteomic analyses of BBMV proteins derived from the midguts of *B. tabaci* and *M. persicae*. In addition, to identification of the most abundant gut surface proteins in each species, we report on the unique and differentially abundant gut plasma membrane proteins from *B. tabaci* and *M. persicae* and discuss bioinformatic predictions of likely plant virus receptors or binding partners.

2 | METHODS

2.1 | Insect rearing

B. tabaci (Hemiptera: Aleyrodidae) Biotype B were reared on cabbage (*Brassica oleracea* var. capitata) in a growth chamber at 26°C with a 14:10 (light:dark) cycle. Whiteflies were passaged weekly to new cabbage plants for

production of newly emerged adults. *M. persicae* colonies were maintained on pepper plants (*Capsicum annuum* cv. California wonder) in an incubator at 26 ± 2°C, with a 14:10 photoperiod (light:dark) and 50 ± 5% relative humidity. Aphids were transferred to new plants every 2 weeks to ensure availability of newly emerged adults.

2.2 | Preparation of BBMV from *B. tabaci* and *M. persicae* adults

Brush border membrane vesicles (BBMV) were prepared according to (Tavares et al., 2022). Guts were dissected under a dissection microscope. BBMVs were prepared from dissected guts via $MgCl_2$ precipitation and differential centrifugation with some modifications (Wolfersberger, 1993). Approximately 2000 *B. tabaci* or 1500 *M. persicae* frozen guts were thawed on ice and transferred into a 3 mL Dounce homogenizer (Wheaton) with 1 mL of cold buffer A (300 mM mannitol, 17 mM Tris HCl pH 7.5, 5 mM ethylene glycol tetraacetic acid-EGTA) supplemented with a 1x protease inhibitor mixture (Pierce™ Protease Inhibitor Tablets, EDTA-free, and propidium iodide [PI]) and 1 mM PMSF (phenylmethylsulphonyl fluoride; Thermo Scientific). Guts were homogenized on ice by 35 strokes. After centrifugation, BBMVs in the pellet were re-extracted with a half volume of buffer A, incubated with $MgCl_2$ and were subjected to a second round of centrifugation (2500*g* for 15 min at 4°C). The resultant supernatant containing BBMV was centrifuged a third time (300,000*g* for 90 min at 4°C, Optima™ TLX Ultracentrifuge). This pellet, now enriched with BBMV, was resuspended in 30 µL of ice-cold buffer A with PI and PMSF (as above), then stored at −80°C. Protein concentration of the prepared BBMV samples was assessed by Nanodrop at 280 nm. As proteins were still present in the supernatant, an additional round of centrifugation was performed (300,000*g* for 90 min at 4°C). The BBMV pellet was resuspended in 15 µL of ice-cold buffer A. BBMV fractions were combined. Three BBMV preparations were made from *B. tabaci* adult guts (2000 guts per replicate: 6000 guts in total) and three from *M. persicae* adult guts (1500 guts per replicate: 4500 guts in total). Each BBMV replicate was prepared separately, with a subsample used for protein concentration and protein enrichment determination. BBMV and crude gut homogenate protein concentrations were determined by Bradford assay with bovine serum albumin (BSA) as a standard (Bradford, 1976). The BBMV protein profile was assessed relative to that of the gut homogenate as follows: samples (2 µg) were solubilized in protein loading buffer (2% sodium dodecyl sulfate [SDS], 10% glycerol, 0.01% bromophenol blue in 60 mmol Tris-HCl buffer), separated by electrophoresis (4%–12% sodium dodecyl sulfate-polyacrylamide gel electrophoresis [SDS-PAGE] gel), and resulting protein bands stained for visualization (Pierce™ Silver Stain for Mass Spectrometry; Thermo Scientific).

2.3 | Sample preparation

SPEED Digestion was performed as described previously (Doellinger et al., 2020; Tavares et al., 2022). BBMVs were solubilized in four volumes of trifluoroacetic acid (TFA; v/v), incubated (2 min at 25°C), neutralized by addition of 10 volumes of 2 M Tris-Base buffer (v/v). To each sample was then added 1.1 volumes of 10X-reduction/alkylation buffer (100 mM Tris[2-carboxyethyl] phosphine [TCEP] 29 mg/mL]/400 mM 2-chloroacetamide [CAA, 37 mg/mL] in H_2O). This mixture was then incubated (5 min, 95°C). The resulting protein concentration (Nanodrop) was adjusted by the addition of dilution buffer (10:1 v/v mixture of 2 M TrisBase and TFA) to a final concentration of 0.25 µg/µL. A 1:50 (w/w; trypsin: sample) ratio was used for trypsin digestion, followed by incubation (37°C, 600 rpm, 20 h in a Thermo Mixer). TFA was added to the resulting trypsin digested peptides to a final concentration of 2%.

2.4 | Desalting of peptides using ZipTip

A micro ZipTip (C18-Ziptip; Millipore) mini-reverse phase (2 µg capacity) was used to desalt peptides resulting from BBMV digestion. A solution of 10 µL of 100% acetonitrile (ACN), 10 µL of 50% ACN/50% of 0.1% trifluoroacetic

acid (TFA) solution was used to equilibrate the ZipTip, followed by three washes with 10 µl of 0.1% TFA. Each suspended peptide sample was pipetted through the ZipTip 10 times. The ZipTip was then washed with TFA 10 times (10 µL of 0.1% each time), and the sample eluted with a solution of 80% ACN/0.1% TFA. The eluted sample was then lyophilized (cold SpeedVac).

2.5 | Mass spectrometry

Samples were separated on a Bruker Fifteen ReproSil (150 mm × 75 µm; 1.9 µm C18) at a flow rate at 400 nL/min with Solvent A (water with 0.1% formic acid [v/v]) and Solvent B (water with 80/20/0.1% ACN/water/formic acid [v/v/v]) on a hybrid trapped ion mobility-quadrupole time-of-flight mass spectrometer (timsTOF fleX; Bruker Daltonics) with a modified nano-electrospray ion source interfaced with an automated Easy nLC 1000 Ultra (Thermo Scientific). Peptides were separated using a linear gradient with Solvent B from 5% to 17% for 60 min, to 25% for 30 min, to 35% for 10 min, to 85% for 10 min, followed by a hold at 85% for 10 more minutes. Data dependent mode with Parallel Accumulation Serial Fragmentation (PASEF) was used to produce the spectrum library to improve ion utilization efficiency and speed of data acquisition. The dual TIMS was operated by the system at a 100% duty cycle, recording the MS/MS mode scans from 100 to 1700 m/z. Ion mobility was scanned from 0.6 to 1.6 Vs/cm^2, at a TIMS ion charge control setting of 5e6. The TIMS dimension was calibrated linearly using four selected ions from the Agilent ESI LC/MS tuning mix (m/z, $1/K_0$: (322.0481, 0.7363 Vs cm^{-2}), (622.0289, 0.9915 Vs cm^{-2}), (922.0097, 1.1996 Vs cm^{-2}), (1221,9906, 1.3934 Vs cm^{-2})] in positive mode.

2.6 | Protein identification

MS/MS tandem spectra extracted by DataAnalysis 5.2 (Bruker) were subjected to a thorough database search (Mascot; Matrix Science; version 2.7.0) against the customized NCBI Refseq databases (O'Leary et al., 2016) for *B. tabaci* (22,737 entries), and *M. persicae* (23,911 entries) with biological modification and amino acid substitution considerations, with a decoy option. Peptide tolerance was set as 10 ppm, tandem MS tolerance ± 0.5 Da, peptide charge of 2+ to 6+, enzyme = trypsin, fixed modification of carbamidomethyl (C), and variable modifications of acetylation and gln->pyro-glu (*N*-terminus), deamidation (N and Q), and oxidation (M). FDR was calculated by Mascot and filtered by Scaffold v4.11.1.

Criteria for protein identification MS/MS based peptide and protein identifications were validated by Scaffold (v4.11.1; Proteome Software Inc.). The threshold for peptide identification acceptance was a > 95.0% probability output from the Scaffold Local FDR algorithm. The threshold for protein identification acceptance was > 99.9% probability (Protein Prophet algorithm; Nesvizhskii et al., 2003), containing at least two identified peptides, and two or more total spectral counts. The principle of parsimony was used to group proteins that contained similar peptides and could not be differentiated solely on MS/MS analysis. Proteins sharing significant peptide similarity were grouped into clusters.

2.7 | Data analysis

A schematic workflow of the data analyses employed for this study is provided in Figure 1. Proteins that localize on the gut surface were predicted with BUSCA (Savojardo et al., 2018), and DeepLoc2 (Almagro Armenteros et al., 2017). Cellular component Gene Ontology terms were predicted by eggNOG5 (Cantalapiedra et al., 2021; Huerta-Cepas et al., 2019). Proteins predicted to be plasma membrane proteins by at least one of these programs were examined for: (1) signal peptides using Phobius (Kall et al., 2007), (2) GPI anchor signals using NetGPIv1.1 (Gíslason et al., 2021) and PredGPI (Pierleoni et al., 2008), (3) transmembrane domain using Phobius (Kall et al., 2007), and (4) palmitoylation

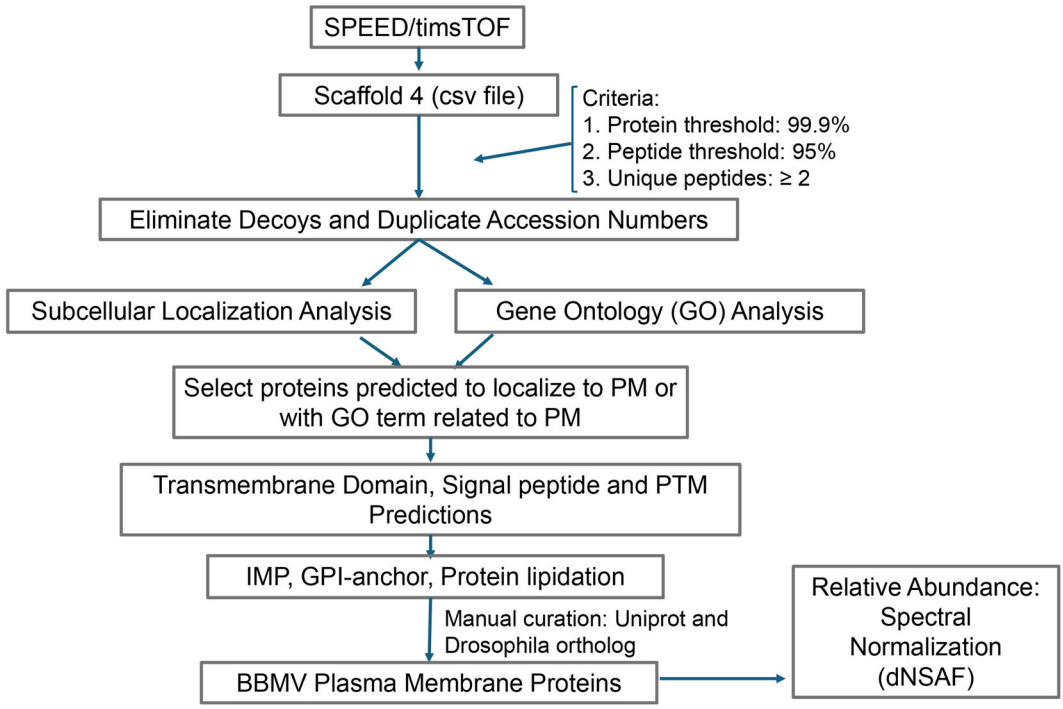

FIGURE 1 Workflow for characterization of protein composition and relative abundance on the midgut epithelium of *Bemisia tabaci* and *Myzus persicae*. BBMV, brush border membrane vesicles.

site using GPS-Palm (Ning et al., 2021). All predicted plasma membrane proteins were then manually checked against the Universal Protein Resource—UniProt database (Bairoch et al., 2005; Wu et al., 2006) and Flybase (Thurmond et al., 2019) to confirm their cellular and gut localization. Proteins predicted to localize to the membrane of organelles were eliminated. Functional annotation of the *B. tabaci* and *M. persicae* gut proteins was performed using DAVID (Huang et al., 2009; Sherman et al., 2022) or eggNOG5 (Cantalapiedra et al., 2021; Huerta-Cepas et al., 2019). For selected gut surface proteins, the number of interacting partners was assessed for orthologous proteins in *Drosophila melanogaster* using the STRING database (Szklarczyk et al., 2023).

Total spectral counts were normalized to the distributed normalized spectral abundance factor (dNSAF) (Zhang et al., 2010). Proteins from *B. tabaci* and *M. persicae* adults were then ranked from higher to lower relative abundance on the gut plasma membrane, and on the gut surface. To determine whether the relative abundance of a protein differed between the two species, we grouped the proteins into those detected in both species, those detected in *B. tabaci* only, and those detected in *M. persicae* only. For proteins found in both insects, we calculated the natural log of each dNSAF following a student *t*-test (*p*-value 0.05) comparison of the ln(dNSAF) from the three technical replicates of *B. tabaci* adults against that of *M. persicae* adults. Spectral count values of zero were replaced with 0.29 to avoid errors during natural log transformation (Zybailov et al., 2006). The R v4.2.3 rstatix package was used for analyses; other data analyses and manipulations used *RStudio* (v. 2021.09.1) tidyverse (Wickham et al., 2019) and seqinr (Charif & Lobry, 2007), or Linux.

To predict likely virus receptors or binding partners from the gut surface proteins identified, we used the GO terms "plasma membrane" (PM; GO:0005886), along with the "protein binding" (GO:0005515), "cell adhesion" (GO:0007155), and "cell surface" (GO.0009986) terms, which were among the most important features determining receptor function according to Valero-Rello et al. (2024). A schematic highlighting the relationship between the GO terms used for this analysis along with their separation into cellular component, biological process or molecular function child terms, is provided in Figure 2 (Binns et al., 2009).

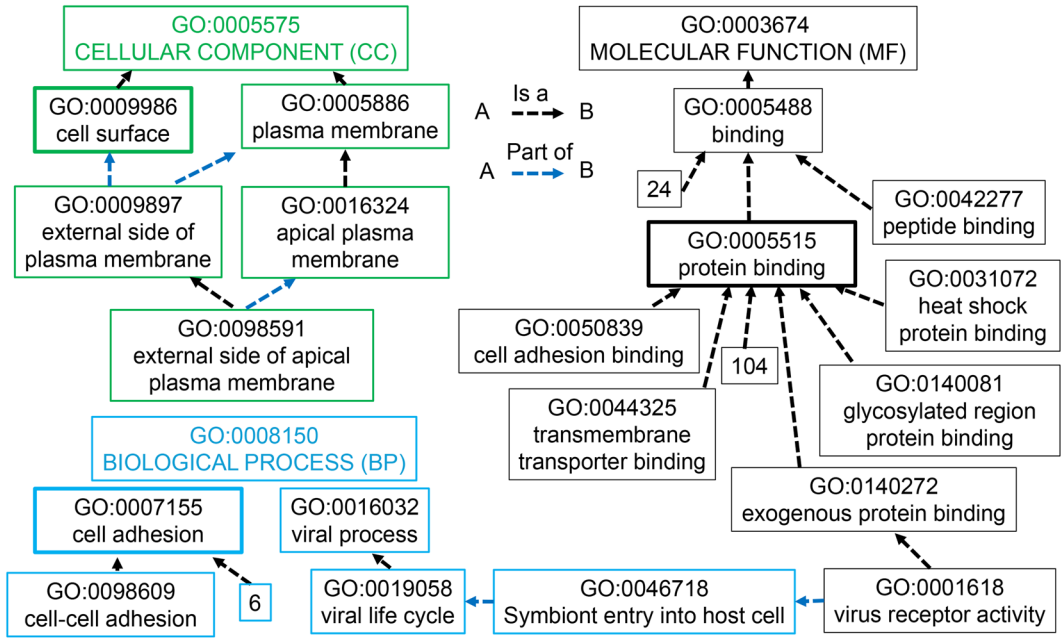

FIGURE 2 Schematic of Gene Ontology (GO) terms associated with viral receptors. All GO terms used for data analysis are depicted with the three primary terms predictive of receptor function in mammals highlighted (cell surface, cell adhesion, protein binding). Biological process (BP) terms are boxed in blue, molecular function (MF) terms in black and cellular component (CC) terms in green. GO term numbers are indicated. Boxed numbers indicate the number of additional child (direct descendant) terms in QuickGo ancestor charts that are not shown (Binns et al., 2009).

3 | RESULTS

3.1 | Proteins identified in *B. tabaci* and *M. persicae* BBMV

BBMV prepared from dissected guts of adult *B. tabaci* and *M. persicae* showed protein profiles typical of BBMV with multiple protein bands in SDS-PAGE gels (Figure S1). While the presence of enriched proteins in the BBMV samples relative to the crude gut homogenate samples is indicative of successful BBMV preparation, the amount of protein loaded in each lane does not appear to be equal based on these gels. Proteomic analysis of BBMV from *B. tabaci* and *M. persicae* adults resulted in the identification of a total of 1699 and 1175 proteins, respectively based on unique accession numbers (Tables S1 and S2). Subcellular localization analysis using DeepLoc2 predicted *B. tabaci* and *M. persicae* BBMV proteins to localize to nine different subcellular compartments, with the major portion predicted to localize to the cytoplasm (48.16% for *B. tabaci* and 41.02% for *M. persicae* BBMV). A portion of 9.37% of *B. tabaci* and 8.43% of *M. persicae* BBMV proteins was predicted to localize to the plasma membrane (Figure 3). In contrast, 22.72% of *B. tabaci* and 21.28% of *M. persicae* proteins were associated with the "plasma membrane" Gene Ontology term (GO:0005886) based on eggNOG5 predictions (Figure 3).

3.2 | Proteins predicted to localize to the plasma membrane of the *B. tabaci* and *M. persicae* gut epithelium cells

We used three different bioinformatic tools (BUSCA, DeepLoc2, and eggNOG5) to predict which proteins localize to the plasma membrane of the midgut epithelium cells. In total, 386 and 250 proteins were predicted to localize to the

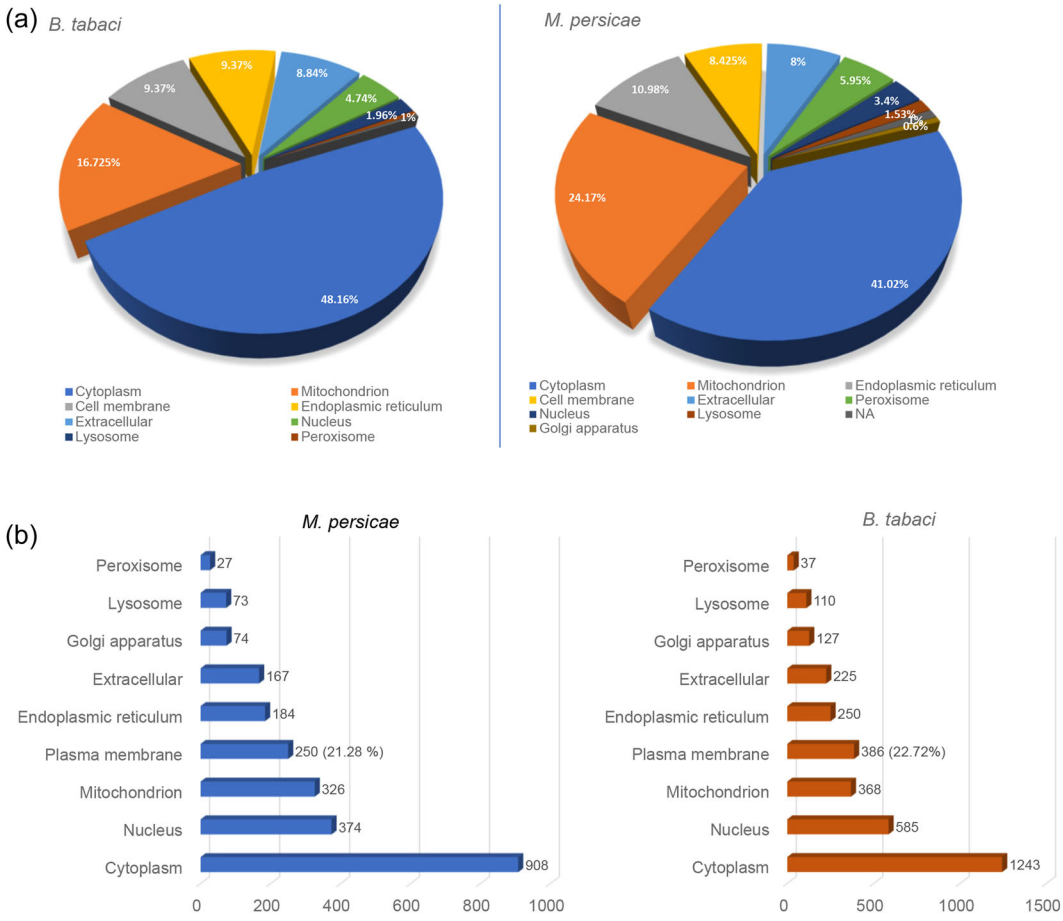

FIGURE 3 Localization of BBMV proteins derived from the midgut epithelial cells of *Bemisia tabaci* and *Myzus persicae*. (a) DeepLoc2 predictions for subcellular localization of BBMV proteins. Arrows indicate the cell membrane category. (b) Gene ontology (GO) cellular component analysis of BBMV proteins by use of eggNOG5. BBMV, brush border membrane vesicles.

plasma membrane of *B. tabaci* and *M. persicae*, respectively (Table S3 and S4). Following careful manual curation and removal of duplicate, identical proteins within species with different accession numbers, a total of 151 and 115 unique plasma membrane proteins were localized to the gut epithelium of *B. tabaci* and *M. persicae*, respectively (Table S5). Among these, 50 were present in both *B. tabaci* and *M. persicae* adult BBMVs based on common orthologs (*D. melanogaster*), and 101 and 65 were only detected in adults of *B. tabaci* or *M. persicae*, respectively (Figure 4).

The relative abundance of plasma membrane proteins in each species are provided in Table S5. Subunits of V-type proton ATPase (of which there are 13), were the most abundant predicted plasma membrane proteins detected for both species. The next most abundant protein in *B. tabaci* was aminopeptidase N (APN) followed by a maltase, and in *M. persicae* was protein l(2)37Cc followed by alkaline phosphatase. Alkaline phosphatase was the 25th most abundant plasma membrane protein in *B. tabaci*. The top 20 most abundant gut surface proteins for *B. tabaci* and *M. persicae* are provided in Table 1.

Following the analysis of Valero-Rello et al. (2024) to identify terms related to virus receptors and binding partners, we used protein binding (GO:0005515), cell adhesion (GO:0007155), and cell surface (GO:0009986), plus the related parent term "biological process" (BP) and child term "molecular function" (MF) associated with virus receptor activity for analysis of the gut plasma membrane proteomes.

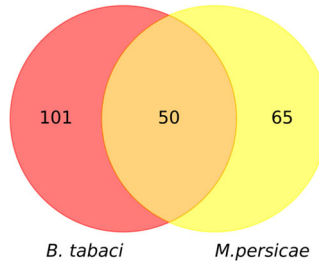

FIGURE 4 *Bemisia tabaci* and *Myzus persicae* proteins predicted to localize to the gut plasma membrane (after manual curation of data).

TABLE 1 The 20 most abundant proteins on the gut surface of *Bemisia tabaci* and *Myzus persicae*.

	Silverleaf whitefly, *B. tabaci*	Green peach aphid, *M. persicae*
1	aminopeptidase N-like isoform X1	protein l(2)37Cc/prohibitin 1
2	maltase A3-like	membrane-bound alkaline phosphatase-like
3	probable maltase isoform X1	aminopeptidase N-like
4	basigin isoform X1	maltase 2-like
5	maltase 2-like	alkaline phosphatase-like
6	prohibitin-2 isoform X2	maltase A1-like
7	alpha-glucosidase-like	maltase A3-like
8	prohibitin-2 isoform X1	multiple inositol polyphosphate phosphatase 1-like isoform X1
9	maltase 1-like	uncharacterized family 31 glucosidase KIAA1161-like
10	alpha-glucosidase-like	flotillin-1
11	alkaline phosphatase-like	V-type proton ATPase 116 kDa subunit a isoform X2
12	maltase A1-like	flotillin-2
13	uncharacterized protein LOC109037465	trehalase-like isoform X1
14	protein 5NUC-like	glutamyl aminopeptidase-like
15	glutamyl aminopeptidase-like isoform X2	leucine-rich repeat-containing protein 55
16	flotillin-2	integrin beta-PS
17	bis(5′-adenosyl)-triphosphatase enpp4-like	fasciclin-1 isoform X1
18	plasma membrane calcium-transporting ATPase 2 isoform X1	monocarboxylate transporter 1 isoform X1
19	flotillin-1	integrin alpha-PS1
20	venom dipeptidyl peptidase 4 isoform X1	G protein alpha q subunit isoform X2

3.2.1 | Protein binding (GO:0005515)

A total of 65 and 51 proteins with the protein binding GO MF term (Figure 2) were predicted to localize to the gut plasma membrane of *B. tabaci and M. persicae* adults, respectively. A total of 26 *B. tabaci* and 25 *M. persicae* proteins from the top 50 most abundant proteins in each species were associated with protein binding (Table S5).

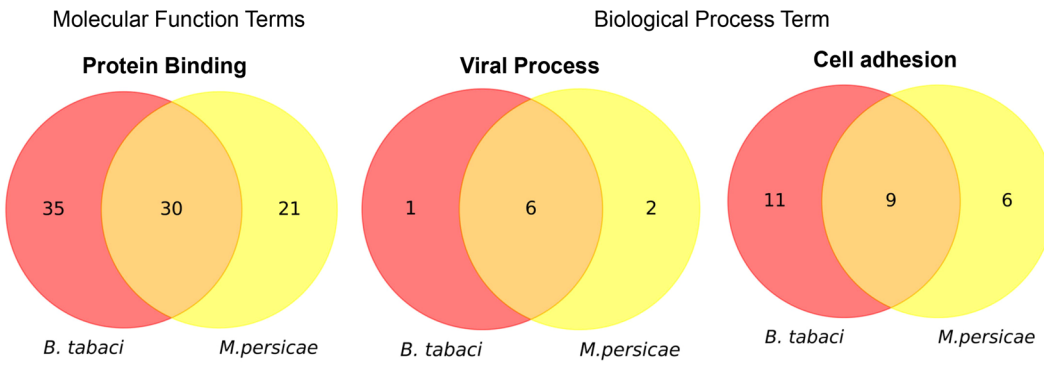

FIGURE 5 *Bemisia tabaci* and *Myzus persicae* gut epithelial membrane proteins associated with the molecular function term protein binding, and the biological process terms viral process and cell adhesion.

Thirty-five *B. tabaci* and 21 *M. persicae* proteins were unique with an additional 30 proteins common to both species (Figure 5).

The top five plasma membrane proteins based on average abundance (dNSAF) that were common to both species in this group were: three V-ATPases, Ras1, and EHD4 (Table S5). The V-ATPases are ATP-dependent proton pumps comprised of 13 subunits that are present in a variety of eukaryotic cellular membranes that mediate acidification of eukaryotic intracellular organelles. Acidification is necessary for intracellular processes such as protein sorting, zymogen activation and receptor-mediated endocytosis (Collins & Forgac, 2020). Receptor-mediated endocytosis is one of the most important processes by which viruses can enter or leave a eukaryotic cell (Gao et al., 2005). Ras 1 proteins are small GTPases that play key roles as molecular switches triggering distinct signal transduction pathways, such as the mitogen-activated protein kinase (MAPK) pathway and the phosphoinositide-3 kinase pathway (Johnson et al., 2000). The MAPK kinase pathway facilitates host defense against viral attack (Mohanta et al., 2020). EHD4 is an Eps15-homology domain containing protein involved in the regulation of endocytotic vesicles (Jones et al., 2020; Okada et al., 2021).

The most abundant proteins related to the protein binding MF term that were unique to *B. tabaci* were moesin/ezrin/radixin homolog 1 (RDX), ras-like GTP-binding protein Rho1 (ROHA), basigin, prohibitin-2, and Na(+)/H(+) exchange regulatory cofactor NHE-RF2 (SLC9A3R2) (Table S5). ROHA belongs to the small GTPase part of the Ras family and plays an important role in entry of bacteria such as *Shigella* and *Salmonella* spp. into mammalian host cells (Jones et al., 1993; Watarai et al., 1997). Basigin is an immunoglobulin domain containing protein involved in *Toxoplasma gondii* (an apicomplexan parasite) infection (Nasuhidehnavi et al., 2022). The protein SLC9A3R2 mediates many cellular processes by binding to and regulating membrane expression and protein-protein interactions of membrane receptors and transport proteins (Stelzer et al., 2016) and is predicted to act in negative regulation of phosphatidylinositol 3-kinase/protein kinase B signal transduction (Drysdale & FlyBase Consortium, 2008; Thurmond et al., 2019). In *M. persicae* the top five most abundant proteins associated with protein binding were protein l(2)37Cc, elongation factor 1-alpha (EEF1A1), stomatin-like protein 2 (STOML2), V-type proton ATPase 116 kDa subunit a, and ras-related protein Rac1 (Table S5).

3.2.2 | Virus receptor activity (GO:0001618) and parent BP terms

In *B. tabaci,* two gut surface proteins, venom dipeptidyl peptidase 4 (DPP4) and xenotropic and polytropic retrovirus receptor 1 homolog (XPR1), were associated with the viral receptor activity MF term (GO:0001618; Figure 2; Table 2). DPP4 is the S9B subfamily of serine peptidases, found widely across organisms (Wu et al., 2023). XPR1 is an inorganic

TABLE 2 Plasma membrane proteins of gut epithelial cells of *Bemisia tabaci* and *Myzus persicae* associated with the viral process GO BP term.

Identifier	Protein name	Mr	Rel. Abund.[a]	Abbr.[b]	PFAMs[c]	Pred-GPI	Net-GPI	TM[d]	SP[e]	Palm[f]
B. tabaci										
XP_018904009.1	V-type proton ATPase subunit H isoform X1	56 kDa	9	ATP6V1H	V-ATPase_H_C,V-ATPase_H_N	N	N	0	N	Y
XP_018907656.1	ras-related protein Rab-5C	23 kDa	18	RAB5A	Ras	N	N	0	N	Y
XP_018905345.1	vesicle-associated membrane protein-associated protein B-like	28 kDa	33	VAPA	Motile_Sperm	N	Y	1	N	N
XP_018898288.1	heat shock protein 83-like	83 kDa	34	HSP90AB1	HATPase_c,HSP90	N	N	0	N	N
XP_018904749.1	venom dipeptidyl peptidase 4 isoform X1 (GO:0001618)	98 kDa	49	DPP4	DPPIV_N,Peptidase_S9	N	N	1	N	Y
XP_018898818.1	integrin beta-PS isoform X2	94 kDa	70	ITGB1	EGF_2,Integrin_B_tail,Integrin_b_cyt,Integrin_beta,P-SI_integrin	N	N	2	N	N
XP_018899350.1	xenotropic and polytropic retrovirus receptor 1 homolog (GO:0001618)	78 kDa	126	XPR1	EXS,SPX	N	N	10	N	Y
M. persicae										
XP_022163711.1	V-type proton ATPase subunit H	55 kDa	10	ATP6V1H	V-ATPase_H_C,V-ATPase_H_N	N	N	0	N	N

(Continues)

TABLE 2 (Continued)

Identifier	Protein name	Mr	Rel. Abund.[a]	Abbr.[b]	PFAMs[c]	Pred-GPI	Net-GPI	TM[d]	SP[e]	Palm[f]
XP_022183700.1	vesicle-associated membrane protein-associated protein A	27 kDa	20	VAPA	Motile_Sperm	N	Y	1	N	N
XP_022160317.1	cdc42 homolog	21 kDa	24	CDC42	Ras	N	N	0	N	Y
XP_022175707.1	heat shock protein 83	83 kDa	25	HSP90AB1	HATPase_c,HSP90	N	N	0	N	N
XP_022178495.1	integrin beta-PS	92 kDa	38	ITGB1	EGF_2,Integrin_B_tail,Integrin_b_cyt,Integrin_beta,PSI_integrin	N	N	1	Y	N
XP_022167683.1	xenotropic and polytropic retrovirus receptor 1-like (GO:0001618)	79 kDa	51	XPR1	EXS,SPX	N	N	7	N	Y
XP_022181507.1	ras-related protein Rab-5C	23 kDa	64	RAB5A	Ras	N	N	0	N	Y
XP_022167059.1	phosphatidylinositol 4-kinase alpha	237 kDa	112	PI4KA	PI3Ka,PI3_PI4_kinase	N	N	0	N	Y

Abbreviations: BP, biological process; GO, Gene Ontology.

[a]Relative abundance of proteins calculated based on the distributed Normalized Spectral Abundance Factor-dNSAF (Zhang et al., 2010).

[b]Protein name abbreviation.

[c]PFAM, protein family.

[d]TM, transmembrane domains predicted by Phobius.

[e]SP, signal peptide predicted by Phobius.

[f]Palm, predicted palmitoylation site (GPS-Palm).

ion transporter that mediates phosphate ion export across the plasma membrane and has an important role in preserving calcium signaling (Bateman et al., 2023). XPR1 enables virus receptor activity acting upstream of- or in response to- virus (Sayers et al., 2021). Of these two proteins, only XPR1 was also detected in *M. persicae* (Table 2).

We further analyzed BBMV plasma membrane proteins associated with both species. Six proteins associated with the BP viral process term (GO:0016032; Figure 2) were common to both species (Figure 5, Table 3, and S5). DPP4 was again detected only in *B. tabaci*, and CDC42 and PI4KA proteins were detected only in *M. persicae* (Table 2). CDC42 belongs to the Rho family of small GTPases and the pool of CDC42 proteins that localizes to the plasma membrane play key roles in polarity and in regulation of the actin cytoskeleton (Farhan & Hsu, 2016). PI4KA catalyzes the first step in the biosynthesis of phosphatidylinositol 4,5-bisphosphate (Sayers et al., 2021) and is important for replication of multiple viruses (Delang et al., 2012).

3.2.3 | Cell adhesion (GO:0007155)

Cell adhesion is a key mechanism that drives the development of multicellular organisms. Cells use adhesion to move, communicate and differentiate, which finally leads to the formation of epithelia and highly organized organs (Mateo et al., 2015). Many cell-adhesion proteins that belong to the immunoglobulin-like superfamily (IgSF CAMs) have been identified as viral receptors in humans (Bhella, 2015; Mateo et al., 2015). There were 20 *B. tabaci* and 15 *M. persicae* plasma membrane proteins associated with the cell adhesion term (GO:0007155) (Figure 5). The top five most abundant *B. tabaci* plasma membrane proteins in this group were: ATP6V1B2, guanine nucleotide-binding protein subunit gamma-1-like, RDX, ROHA and basigin. The most abundant *M. persicae* proteins related to cell adhesion were ATP6V1B2, guanine nucleotide-binding protein subunit gamma-1-like, CDC42, RAC2, flotillin-1, and integrin beta-PS (Table S5).

3.2.4 | Plasma membrane and cell surface associated GO terms

In *B. tabaci* 15, 32, and 116 BBMV proteins were associated with the cell surface (GO:0009986), apical plasma membrane (GO:0016324) and plasma membrane (GO:0005886) GO terms, respectively (Figure 2 and Table S5). In the *M. persicae* BBMV proteome, 16, 15, and 90 proteins related to cell surface, apical plasma membrane and plasma membrane terms were identified, respectively (Table S5). The top three proteins associated with the cell surface term in *B. tabaci* were: RDX, basigin and prohibitin-2 (Table S5). In *M. persicae*, they were protein l(2)37Cc, membrane-bound alkaline phosphatase, and ras-related protein Ral-a protein.

3.3 | In silico characterization of uncharacterized proteins predicted to localize to the plasma membrane

Nine *B. tabaci* and seven *M. persicae* uncharacterized BBMV proteins were predicted to localize to the plasma membrane (Table S6). The eggNOG5 prediction tool was used to characterize these proteins based on domain information, GO and KEGG pathway terms. The top three most abundant uncharacterized proteins in *B. tabaci* have major facilitator superfamily (MFS_1) domains (Table S6). The major facilitator superfamily (MFS) of membrane proteins represents the largest family of secondary transporters. MFS proteins target a wide spectrum of substrates, including ions, carbohydrates, lipids, amino acids and peptides, nucleosides, and other small molecules in both directions across the membrane (Letunic et al., 2021). In *M. persicae*, some of the uncharacterized predicted plasma membrane proteins have ERAP1_C, peptidase_M1, AMP-binding, and MFS_1 domains (Table S6). Peptidase_M1 is present in metallopeptidase families. This group of metallopeptidases belong to the MEROPS peptidase family M1 (clan MA(E)), the type example being aminopeptidase N (Letunic et al., 2021). ERAP1_C domain

TABLE 3 Plasma membrane gut epithelial cell proteins that significantly differ in abundance in *Bemisia tabaci* (Bt) and *Myzus persicae* (Mp).

Predicted *B. tabaci* protein	Mr	Identifier	*M. persicae* protein	Mr	Rel. Abund. Bt [a]	Rel. Abund Mp [a]	*p*_Value	More in	Average dNSAF.x	Average dNSAF.y
Vesicle-associated membrane protein-associated protein B-like (VAPA)	28 kDa	XP_022183700.1	Vesicle-associated membrane protein-associated protein A	27 kDa	33	20	0.0369*	Mp	0.005819813	0.014106126
Fasciclin-2-like (NCAM2)	95 kDa	XP_022172974.1	Fasciclin-2, partial	96 kDa	74	105	0.0291*	Bt	0.002208345	6.69E-04
Xenotropic and polytropic retrovirus receptor 1 homolog (XPR1)	78 kDa	XP_022167683.1	Xenotropic and polytropic retrovirus receptor 1-like	79 kDa	126	51	0.0188*	Mp	9.01E-04	0.003095802
Alkaline phosphatase-like	61 kDa	XP_022175115.1	Alkaline phosphatase-like	64 kDa	25	13	0.0107*	Mp	0.007148538	0.018557072
V-type proton ATPase subunit H isoform X1 (ATP6V1H)	56 kDa	XP_022163711.1	V-type proton ATPase subunit H	55 kDa	9	10	0.0104*	Mp	0.014667905	0.020968253
Complement component 1 Q subcomponent-binding protein, mitochondrial isoform X1 (C1QBP)	31 kDa	XP_022164081.1	Complement component 1 Q subcomponent-binding protein, mitochondrial	28 kDa	45	23	0.0195*	Mp	0.004286563	0.011263245
V-type proton ATPase subunit C (ATP6V1C2)	44 kDa	XP_022180732.1	V-type proton ATPase subunit C	44 kDa	7	7	0.0493*	Mp	0.015239356	0.029644004
Metal transporter CNNM4-like isoform X1 (CNNM@)	97 kDa	XP_022166382.1	Metal transporter CNNM4 isoform X2	107 kDa	59	80	0.0321*	Bt	0.003345294	0.001654274
ATP-binding cassette sub-family A member 2-like	185 kDa	XP_022171731.1	ATP-binding cassette sub-family A member 3-like	198 kDa	67	106	0.00832**	Bt	0.002446935	6.05E-04
Ras-related protein Rab-35	23 kDa	XP_022174425.1	Ras-related protein Rab-35	23 kDa	68	41	0.00411**	Mp	0.00242476	0.00422916

[a]Relative abundance of proteins calculated based on the distributed Normalized Spectral Abundance Factor-dNSAF (Zhang et al., 2010).

is also present in APN and is composed of 16 alpha helices organized as 8 HEAT-like repeats (Letunic et al., 2021). The AMP-binding domain, also identified in one of the uncharacterized proteins, is Ser/Thr/Gly-rich and is further characterized by a conserved Pro-Lys-Gly triplet (Letunic et al., 2021).

3.4 | Relative abundance and differences between the adult *B. tabaci* and *M. persicae* gut plasma membrane proteomes

Gut plasma membrane proteins associated with the BBMV derived from adults of both insects were ranked from high to low relative abundance based on their average dNSAF (Table S5). The order of abundance differed between adults of *B. tabaci* and *M. persicae*.

Statistical analyses were performed for interspecies comparison of BBMV proteins that were predicted to localize to the plasma membrane and were orthologous. In total, 50 detected BBMV proteins (< 50%) have common orthologs among these two insects (Table S7). The abundance of 10 proteins differed significantly between *B. tabaci* and *M. persicae*. Out of these, seven were more abundant in *M. persicae* and three were more abundant in *B. tabaci* (Table 3). The three proteins (VAPA, XPR1, and ATP6V1H) that were more abundant in *M. persicae* were associated with the viral process GO term (Table 2). Fasciclin-2, a cell adhesion protein, was more abundant in *B. tabaci*, and the other three proteins that were more abundant in *B. tabaci* were associated with the cell surface GO term (Table 3).

3.5 | Analysis of features predictive of receptor function

Features predictive of receptor function were examined for eight proteins selected on the basis of (1) known receptor function for pathogens or bacteria-derived pesticidal proteins in insects, and/or (2) abundance in *B. tabaci* and *M. persicae* (Table 4). Of these, only the *B. tabaci* fasciclin-2-like protein met all four criteria: GO terms protein binding, cell adhesion, cell surface, and multiple interacting partners. The cell surface GO term did not apply to *M. persicae* fasciclin-1 isoform X1. Similarly DE-cadherin and prohibitin homologs from both species met three of the four criteria, all except the cell surface GO term. Aminopeptidase N, while interacting with multiple proteins, did not meet any of the GO terms employed for prediction of virus receptor function in mammals. However, all eight proteins met at least one GO term criterion when peptide binding (GO:0042277, Figure 2) and plasma membrane (GO:0005886) were considered, apart from *M. persicae* facilitated trehalose transporter Tret1-2 homolog isoform X3 (Table 4).

4 | DISCUSSION

We characterized the gut plasma membrane proteomes of *B. tabaci* and *M. persicae* adults to identify the most abundant gut surface proteins, which represent potential binding partners of circulative viruses vectored by these two insects. A total of 151 and 115 unique gut plasma membrane proteins were detected in *B. tabaci and M. persicae* BBMV proteome, respectively. We identified 50 unique plasma membrane proteins common to the two species based on common orthologs (*D. melanogaster*), of which 10 differ in abundance between the two species and identified the most abundant gut surface proteins in the two hemipteran species.

4.1 | *B. tabaci* and *M. persicae* and other insect BBMV proteomes

The proteome of BBMV allows us to determine the composition and abundance of proteins on the gut surface. However, remnant proteins of the cytosol and cellular organelles represent a significant proportion of the total. In

TABLE 4 Gut surface proteins that share common terms associated with viral receptors.

Identifier	Proteins	Orthologs in *Drosophila melanogaster*	Rel. Abund.[a]	Protein binding[b]	Peptide binding[c]	Cell adhesion[d]	Cell surface[e]	Plasma membrane[f]	No. interactors[g]
Bemisia tabaci	PREDICTED:								
XP_018896627.1	Aminopeptidase N-like isoform X1	FBpp0084751	4	No	Yes	No	No	No	12
XP_018898449.1	Glutamyl aminopeptidase-like isoform X2	**FBpp0082209**; FBpp0082211; FBpp0288476	31	No	Yes	No	Yes	Yes	14
XP_018902336.1	Facilitated trehalose transporter Tret1-2 homolog isoform X1	**FBpp0075674**; FBpp0082790; FBpp0086060; FBpp0088616	62	No	No	No	No	Yes	3
XP_018914109.1	Alkaline phosphatase-like	**FBpp0076794**; FBpp0076835; FBpp0081538; FBpp0083450; FBpp0087603	25	No	No	No	Yes	No	6
XP_018895757.1	Maltase 2-like	**FBpp0079859**; FBpp0079860; FBpp0087827; FBpp0087828; FBpp0087831; FBpp0087836; FBpp0087837; FBpp0087838; FBpp0271830	14	No	No	No	No	Yes	4
XP_018906343.1	Prohibitin-2 isoform X2	FBpp0111775	17	Yes	No	No	Yes	No	28
XP_018899969.1	Fasciclin-2-like	FBpp0070633	74	Yes	No	Yes	Yes	Yes	16
XP_018909178.1	DE-cadherin	FBpp0071475	132	Yes	No	Yes	No	Yes	50
Myzus persicae									
XP_022165263.1	Aminopeptidase N-like	**FBpp0071421**; FBpp0071435; FBpp0075867; FBpp0271735; FBpp0297620	11	No	Yes	No	No	No	12

TABLE 4 (Continued)

Identifier	Proteins	Orthologs in *Drosophila melanogaster*	Rel. Abund.[a]	Protein binding[b]	Peptide binding[c]	Cell adhesion[d]	Cell surface[e]	Plasma membrane[f]	No. interactors[g]
XP_022175105.1	Membrane-bound alkaline phosphatase-like	**FBpp0076794**; FBpp0076835; FBpp0081538; FBpp0083450; FBpp0087603	8	No	No	No	Yes	No	6
XP_022182397.1	Facilitated trehalose transporter Tret1-2 homolog isoform X3	FBpp0078291	50	No	No	No	No	No	0
XP_022171483.1	Maltase 2-like	**FBpp0079859**; FBpp0079860; FBpp0087827FBpp0087828; FBpp0087831; FBpp0087836 FBpp0087837; FBpp0087838; FBpp0271830	12	No	No	No	No	Yes	4
XP_022178106.1	Protein l(2)37 Cc (Prohibitin homologue)	FBpp0080707	5	Yes	No	No	Yes	Yes	12
XP_022176858.1	Fasciclin-1 isoform X1	FBpp0111715	42	Yes	No	Yes	No	Yes	3
XP_022166977.1	DE-cadherin	FBpp0071475	66	Yes	No	Yes	No	Yes	50

[a]Relative abundance of proteins calculated based on the distributed Normalized Spectral Abundance Factor-dNSAF (Zhang et al., 2010).

[b]Proteins with GO terms protein binding (GO:0005515),

[c]peptide binding (GO:0042277),

[d]Cell adhesion (GO:0007155),

[e]cell surface GO (GO:0009986),

[f]plasma membrane (GO:0005886) are indicated.

[g]Number of interacting partners predicted at high confidence (> 0.7) at sting-db.org; accessed April 11, 2024. For proteins with multiple orthologs in *D. melanogaster*, the number of interacting partners is shown for the ortholog in bold.

similar studies, only aproximately 7% of BBMV proteins were predicted to localize to the gut surface of *D. citri* and *T. ni* (Javed et al., 2019; Tavares et al., 2022). The percentage of gut surface proteins identified in these two studies was based on unique accession numbers (not unique proteins). In the current study, subcellular localization tools were used in conjunction with GO, posttranslational, and signal peptide transmembrane helix/domain prediction tools. The combination of tools used increased both the number of proteins identified and the percentage of proteins predicted to localize to the plasma membrane of gut epithelial cells. After careful manual curation and removal of duplicate proteins (i.e., identical proteins with different accession numbers), 8.95% and 9.8% proteins localized to the gut cell membrane of *B. tabaci* and *M. persicae*, respectively. The manual curation step is essential: more than half of the proteins initially predicted to be on the plasma membrane of *B. tabaci* and *M. persicae* (Tables S1–S5) were not predicted to localize to the gut epithelium following manual curation. Use of GO analysis in conjunction with cellular localization prediction increased the number of predicted plasma membrane proteins to 21%–23%. In *Aedes aegypti*, bioinformatic analysis alone predicted that 26% out of 246 proteins identified from BBMV lipid rafts localized to the plasma membrane (Bayyareddy et al., 2012). This high percentage of plasma membrane proteins reflects the use of the lipid raft-enriched fraction rather than total BBMV for their study. While proteomic analyses of other insect-derived BBMV have been described (Ma et al., 2012; Pauchet et al., 2009; Popova-Butler & Dean, 2009; Yuan et al., 2011), these studies did not focus on proteins present on the luminal surface.

4.2 | Comparison between the gut plasma membrane proteomes of *B. tabaci* and *M. persicae* adults

This is the first study to directly compare the gut plasma membrane proteomes of two different insect species. V-type proton ATPase was the most abundant gut plasma membrane protein in both cases with most of the protein subunits being intracellular. In comparison to *D. citri*, where alkaline phosphatase and aminopeptidase N were the most abundant proteins on the gut surface (Tavares et al., 2022), aminopeptidase N proteins were ranked 1 and 15 for *B. tabaci* and 3 and 14 for *M. persicae* (Table 1). Alkaline phosphatase proteins were the second and fifth most abundant gut surface proteins in *M. persicae*, and the eleventh most abundant gut surface proteins in *B. tabaci* within the top 20 (Table 1). Prohibitin 1 was the most abundant gut surface protein in *M. persicae*, and prohibitin 2 isoforms ranked 6 and 8 in relative abundance in *B. tabaci*. Prohibitin is a multifunctional protein with a small extracullar domain when located in the plasma membrane (Villegas-Coronado et al., 2022). Taken together, these proteins along with alpha-amylase enzymes (maltase, alpha glucosidase) clearly play key roles on the hemipteran gut surface. All three proteins (aminopeptidase N, alkaline phosphatase, alpha-amylase enzymes) are known to be exploited for binding (Jurat-Fuentes et al., 2021) or entry into the host by plant or insect pathogens in these or in other insects.

A subset of proteins that were only detected in the adults of *B. tabaci* (101) or *M. persicae* (65) were mostly of low abundance. These low abundance proteins may have been lost in these cases during protein solubilization (detergent based or detergent free (SPEED) methods and separation (reverse phase or HILIC column-based), rather than being absent from the respective species, highlighting a potential limitation of the protocols employed.

4.3 | Virus receptors and binding partners

Candidate plant virus receptors, namely the cubilin and amnionless receptor complex in *B. tabaci* (Zhao et al., 2020), and ephrin in *M. persicae* (Mulot et al., 2018) are associated with protein binding in hemipterans. Cubilin, amnionless and ephrin proteins were not detected in the BBMV gut proteome of *B. tabaci* and *M. persicae* however. The lack of detection suggests that either these proteins have low abundance, only transiently localize to the gut surface (e.g., based on posttranslational modification) or were underrepresented due to the protein extraction method employed in the current study. An alternative scenario is that these proteins do not function as viral cell surface receptors. In

contrast, aminopeptidase N was among the most abundant gut surface proteins in both *B. tabaci* and *M. persicae*. This protein is a candidate receptor for the begomovirus, TYLCV in *B. tabaci* (Fan et al., 2024) and has been definitively demonstrated to function as a receptor for the luteovirus, *Pea enation mosaic virus* in the pea aphid, *Acyrthosiphon pisum* (Linz et al., 2015; Liu et al., 2010).

Recent studies have implicated several additional gut epithelial plasma membrane proteins as binding partners for circulative viruses in *B. tabaci* or *M. persicae*. First, vesicle-associated membrane protein-associated protein B (VAPB) was identified as a binding partner of TYLCV in *B. tabaci* (Zhao et al., 2019). This protein was present in the *B. tabaci* gut surface proteome, is associated with the protein binding GO term and possesses an immunoglobulin (Ig)-like_fold. Second, the complement component 1 Q subcomponent binding protein (C1QBP) is a glycoprotein that binds to the coat protein of the polerovirus *Pepper whitefly-borne vein yellows virus*, in *B. tabaci* (Ghosh et al., 2021). C1QBP was also identified in *M. persicae* as a binding partner of another polerovirus, *Potato leafroll virus* (DeBlasio et al., 2021). C1QBP was identified in this study in both hemipteran insect gut surface proteomes and is associated with the protein binding and cell surface terms. Third, V-type proton ATPase subunit D and guanine nucleotide-binding protein subunit gamma-1 were among proteins identified from a yeast two-hybrid screen for proteins that interact with the readthrough protein of *Barley yellow dwarf virus-GPV* (Wang et al., 2015). The protein binding and transporter activity GO MF terms were prioritized in their data analyses (Wang et al., 2015). V-type proton ATPase subunit D was among the top 20 most abundant proteins in our *M. persicae* gut plasma membrane proteome, and guanine nucleotide-binding protein subunit gamma-1 was among the 20 most abundant proteins for both species (Table S5).

None of the four proteins implicated in binding to circulative viruses described above have been shown to function as gut surface receptors, however. Indeed, the use of homogenized tissues (rather than BBMV), and the yeast two-hybrid system to study protein-protein interactions increases the chance of false positive interactions, particularly for proteins that do not co-localize under in vivo conditions. This is particularly true for proteins that function through protein binding (e.g. chaperones). The specific roles of the putative virus binding proteins in the biology of these plant viruses in their insect vectors remain to be definitively elucidated.

The GO terms protein binding, cell adhesion, and cell surface along with the number of interacting partners were optimal for prediction of cell surface receptor function in mammals (Valero-Rello et al., 2024). Our analysis of selected proteins with respect to these criteria along with the related GO terms (plasma membrane, peptide binding) suggests that the same model may apply to insect gut surface proteins: The two confirmed plant virus receptors in Hemiptera are aminopeptidase N in the pea aphid, *A. pisum* (Linz et al., 2015) and sugar transporter 6 (a Tret1-2 homolog; Table 4) in the small brown planthopper, *Laodelphax striatellus* (Qin et al., 2018). Glutamyl-aminopeptidase-like was characterized by three predictive features of mammalian cell receptors plus multiple interacting partners and the Tret1-2 homolog was associated with one predictive feature in *B. tabaci*. Cadherin and alkaline phosphatase (in addition to aminopeptidase N), are known receptors that mediate binding and pore formation by bacteria-derived pesticidal proteins (Jurat-Fuentes et al., 2021). Most mammalian cell receptor predictive features apply to cadherin, and the others (cell surface) to alkaline phosphatase. The predicted fasciclin-2-like protein of *B. tabaci* met all four criteria suggesting that this protein may warrant further attention as a candidate plant virus receptor. However, the number of interacting partners was the most important predictive feature for receptor function in the prior study (Valero-Rello et al., 2024). Given the paucity of gut receptor proteins definitively identified for any insect pathogen or insect vectored pathogen (Bonning, 2025), whether pathogens exploit the most abundant gut surface proteins-, and whether plant viruses exploit multiple receptor proteins in the same or in different insect vectors- are questions that both remain to be addressed.

5 | CONCLUSIONS

We present the first comprehensive profile of the midgut plasma membrane proteome for adult *B. tabaci* and *M. persicae*, two of the most important hemipteran vectors of plant viruses. Alkaline phosphatase, aminopeptidase N and maltase were abundant gut surface proteins in both species, all three of which are targeted by pathogens in

other insects. While the composition of proteins on the gut plasma membrane was similar between the two species, 10 proteins differed in abundance. Bioinformatics analysis to identify gut surface proteins likely to function as virus receptors based on a mammalian virus receptor model, highlighted *B. tabaci* fasciclin and cadherin as proteins with high potential for receptor functionality.

AUTHOR CONTRIBUTIONS

Jaime Jiménez: Conceptualization; investigation; methodology; validation; writing—review & editing. **Ruchir Mishra**: Conceptualization; data curation; formal analysis; validation; visualization; writing—original draft. **Xinyue Wang**: Investigation; methodology. **Ciara M. Magee**: Investigation; methodology. **Bryony C. Bonning**: Conceptualization; funding acquisition; project administration; supervision; visualization; writing—review & editing.

ACKNOWLEDGMENTS

The authors thank Dr. Jane E. Polston, University of Florida for provision of whitefly and aphid colonies and K. Grace Crummer for critical reading of the manuscript. This material is based upon work supported by the National Science Foundation IUCRC, the Center for Arthropod Management Technologies under Grant Nos. IIP-1821914 and 2310815, and by industry partners.

CONFLICT OF INTEREST STATEMENT

The authors declare no conflict of interest.

DATA AVAILABILITY STATEMENT

Scaffold files available at https://figshare.com/s/3f9c97bda1cd343eaf75: PM967, PM974, PM975: *M. persicae* Scaffold files (.sf3): Three biological replicates ICBR-PM-965-976-999: *B. tabaci* Scaffold files (.sf3): Three biological replicates.

ORCID

Jaime Jiménez https://orcid.org/0000-0002-1359-9070
Ruchir Mishra https://orcid.org/0009-0003-5938-8409
Xinyue Wang https://orcid.org/0009-0006-8957-3877
Ciara M. Magee https://orcid.org/0009-0003-3426-3570
Bryony C. Bonning http://orcid.org/0000-0002-9956-9613

REFERENCES

Almagro Armenteros, J.J., Sønderby, C.K., Sønderby, S.K., Nielsen, H. & Winther, O. (2017) DeepLoc: prediction of protein subcellular localization using deep learning. *Bioinformatics*, 33, 3387–3395.

Bairoch, A. (2004) The universal protein resource (UniProt). *Nucleic Acids Research*, 33, D154–D159.

Bateman, A., Martin, M.J., Orchard, S., Magrane, M., Ahmad, S., Alpi, E. et al.The UniProt Consortium. (2023) UniProt: the universal protein knowledgebase in 2023. *Nucleic Acids Research*, 51, D523–D531. Available from: https://doi.org/10.1093/nar/gkac1052

Bayyareddy, K., Zhu, X., Orlando, R. & Adang, M.J. (2012) Proteome analysis of Cry4Ba toxin-interacting *Aedes aegypti* lipid rafts using geLC–MS/MS. *Journal of Proteome Research*, 11, 5843–5855.

Bhella, D. (2015) The role of cellular adhesion molecules in virus attachment and entry. *Philosophical Transactions of the Royal Society, B: Biological Sciences*, 370, 20140035. Available from: https://doi.org/10.1098/rstb.2014.0035

Binns, D., Dimmer, E., Huntley, R., Barrell, D., O'Donovan, C. & Apweiler, R. (2009) QuickGO: a web-based tool for gene ontology searching. *Bioinformatics*, 25, 3045–3046.

Blackman, R.L. & Eastop, V.F. (2000) *Aphids on the world's crops: an identification and information guide*, 2nd edition. Hoboken: Wiley.

Bonning, B.C. (2025) Pathogen binding and entry: molecular interactions with the insect gut. *Annual Review of Entomology*. Forthcoming.

Bradford, M.M. (1976) A rapid and sensitive method for the quantitation of microgram quantities of protein utilizing the principle of protein-dye binding. *Analytical Biochemistry*, 72, 248–254.

Butt, A.H., Rasool, N. & Khan, Y.D. (2017) A treatise to computational approaches towards prediction of membrane protein and its subtypes. *The Journal of Membrane Biology*, 250, 55–76.

Caccia, S., Casartelli, M. & Tettamanti, G. (2019) The amazing complexity of insect midgut cells: types, peculiarities, and functions. *Cell and Tissue Research*, 377, 505–525.

Cantalapiedra, C.P., Hernández-Plaza, A., Letunic, I., Bork, P. & Huerta-Cepas, J. (2021) eggNOG-mapper v2: functional annotation, orthology assignments, and domain prediction at the metagenomic scale. *Molecular Biology and Evolution*, 38, 5825–5829.

Charif, D. & Lobry, J.R. (2007) SeqinR 1.0-2: a contributed package to the R project for statistical computing devoted to biological sequences retrieval and analysis. In: Bastolla, U., Porto, M., Roman, H.E. & Vendruscolo, M., (Eds.) *Structural approaches to sequence evolution: molecules, networks, populations*. Berlin, Heidelberg: Springer. pp. 207–232 in: https://doi.org/10.1007/978-3-540-35306-5_10

Collins, M.P. & Forgac, M. (2020) Regulation and function of V-ATPases in physiology and disease. *Biochimica et Biophysica Acta (BBA) - Biomembranes*, 1862, 183341. Available from: https://doi.org/10.1016/j.bbamem.2020.183341

Czosnek, H., Hariton-Shalev, A., Sobol, I., Gorovits, R. & Ghanim, M. (2017) The incredible journey of begomoviruses in their whitefly vector. *Viruses*, 9, 273.

DeBlasio, S.L., Wilson, J.R., Tamborindeguy, C., Johnson, R.S., Pinheiro, P.V., MacCoss, M.J. et al. (2021) Affinity purification–mass spectrometry identifies a novel interaction between a polerovirus and a conserved innate immunity aphid protein that regulates transmission efficiency. *Journal of Proteome Research*, 20, 3365–3387. Available from: https://doi.org/10.1021/acs.jproteome.1c00313

Delang, L., Paeshuyse, J. & Neyts, J. (2012) The role of phosphatidylinositol 4-kinases and phosphatidylinositol 4-phosphate during viral replication. *Biochemical Pharmacology*, 84, 1400–1408. Available from: https://doi.org/10.1016/j.bcp.2012.07.034

Doellinger, J., Schneider, A., Hoeller, M. & Lasch, P. (2020) Sample preparation by easy extraction and digestion (SPEED)-a universal, rapid, and detergent-free protocol for proteomics based on acid extraction. *Molecular & Cellular Proteomics*, 19, 209–222.

Drysdale, R., FlyBase Consortium. (2008) FlyBase: a database for the Drosophila research community. *Methods in Molecular Biology*, 420, 45–59. Available from: https://doi.org/10.1007/978-1-59745-583-1_3

Fan, Y.-Y., Chi, Y., Chen, N., Cuellar, W.J. & Wang, X.-W. (2024) Role of aminopeptidase N-like in the acquisition of begomoviruses by Bemisia tabaci, the whitefly vector. *Insect Science*, 31(3), 707–719. https://doi.org/10.1111/1744-7917.13336

Farhan, H. & Hsu, V.W. (2016) Cdc42 and cellular polarity: emerging roles at the Golgi. *Trends in Cell Biology*, 26, 241–248. Available from: https://doi.org/10.1016/j.tcb.2015.11.003

Fereres, A. & Raccah, B. (2015) Plant virus transmission by insects, *Encyclopedia of Life Sciences*. John Wiley & Sons, Ltd. pp. 1–12. https://doi.org/10.1002/9780470015902.a0000760.pub3

Gao, H., Shi, W. & Freund, L.B. (2005) Mechanics of receptor-mediated endocytosis. *Proceedings of the National Academy of Sciences of the United States of America*, 102, 9469–9474. Available from: https://doi.org/10.1073/pnas.0503879102

Ghosh, S., Bello, V.H. & Ghanim, M. (2021) Transmission parameters of pepper whitefly-borne vein yellows virus (PeWBVYV) by *Bemisia tabaci* and identification of an insect protein with a putative role in polerovirus transmission. *Virology*, 560, 54–65.

Ghosh, S. & Ghanim, M. (2021) Factors determining transmission of persistent viruses by *Bemisia tabaci* and emergence of new virus–vector relationships. *Viruses*, 13, 1808.

Gíslason, M.H., Nielsen, H., Almagro Armenteros, J.J. & Johansen, A.R. (2021) Prediction of GPI-anchored proteins with pointer neural networks. *Current Research in Biotechnology*, 3, 6–13.

Gray, S. & Gildow, F.E. (2003) Luteovirus-aphid interactions. *Annual Review of Phytopathology*, 41, 539–566. Available from: https://doi.org/10.1146/annurev.phyto.41.012203.105815

Hogenhout, S.A., Ammar, E.-D., Whitfield, A.E. & Redinbaugh, M.G. (2008) Insect vector interactions with persistently transmitted viruses. *Annual Review of Phytopathology*, 46, 327–359. Available from: https://doi.org/10.1146/annurev.phyto.022508.092135

Holtof, M., Lenaerts, C., Cullen, D. & Vanden Broeck, J. (2019) Extracellular nutrient digestion and absorption in the insect gut. *Cell and Tissue Research*, 377, 397–414.

Huang, D.W., Sherman, B.T. & Lempicki, R.A. (2009) Systematic and integrative analysis of large gene lists using DAVID bioinformatics resources. *Nature Protocols*, 4, 44–57.

Huerta-Cepas, J., Szklarczyk, D., Heller, D., Hernández-Plaza, A., Forslund, S.K., Cook, H. et al. (2019) eggNOG 5.0: a hierarchical, functionally and phylogenetically annotated orthology resource based on 5090 organisms and 2502 viruses. *Nucleic Acids Research*, 47, D309–D314.

Javed, M.A., Coutu, C., Theilmann, D.A., Erlandson, M.A. & Hegedus, D.D. (2019) Proteomics analysis of *Trichoplusia ni* midgut epithelial cell brush border membrane vesicles. *Insect science*, 26, 424–440.

Johnson, S.A.S., Mandavia, N., Wang, H.-D. & Johnson, D.L. (2000) Transcriptional regulation of the TATA-binding protein by ras cellular signaling. *Molecular and Cellular Biology*, 20, 5000–5009. Available from: https://doi.org/10.1128/MCB.20.14.5000-5009.2000

Jones, B.D., Paterson, H.F., Hall, A. & Falkow, S. (1993) *Salmonella typhimurium* induces membrane ruffling by a growth factor-receptor-independent mechanism. *Proceedings of the National Academy of Sciences of the United States of America*, 90, 10390–10394. Available from: https://doi.org/10.1073/pnas.90.21.10390

Jones, T., Naslavsky, N. & Caplan, S. (2020) Eps15 homology domain protein 4 (EHD4) is required for Eps15 homology domain protein 1 (EHD1)-mediated endosomal recruitment and fission. *PLoS One*, 15, e0239657. Available from: https://doi.org/10.1371/journal.pone.0239657

Jurat-Fuentes, J.L., Heckel, D.G. & Ferré, J. (2021) Mechanisms of resistance to insecticidal proteins from *Bacillus thuringiensis*. *Annual Review of Entomology*, 66, 121–140. Available from: https://doi.org/10.1146/annurev-ento-052620-073348

Kall, L., Krogh, A. & Sonnhammer, E.L.L. (2007) Advantages of combined transmembrane topology and signal peptide prediction—the Phobius web server. *Nucleic Acids Research*, 35, W429–W432.

Letunic, I., Khedkar, S. & Bork, P. (2021) SMART: recent updates, new developments and status in 2020. *Nucleic Acids Research*, 49, D458–D460. Available from: https://doi.org/10.1093/nar/gkaa937

Linz, L.B., Liu, S., Chougule, N.P. & Bonning, B.C. (2015) In vitro evidence supports membrane alanyl aminopeptidase N as a receptor for a plant virus in the pea aphid vector. *Journal of Virology*, 89, 11203–11212. Available from: https://doi.org/10.1128/JVI.01479-15

Liu, S., Sivakumar, S., Sparks, W.O., Miller, W.A. & Bonning, B.C. (2010) A peptide that binds the pea aphid gut impedes entry of pea enation mosaic virus into the aphid hemocoel. *Virology*, 401, 107–116. Available from: https://doi.org/10.1016/j.virol.2010.02.009

Ma, W., Zhang, Z., Peng, C., Wang, X., Li, F. & Lin, Y. (2012) Exploring the midgut transcriptome and brush border membrane vesicle proteome of the rice stem borer, *Chilo suppressalis* (Walker). *PLoS One*, 7, e38151.

Mateo, M., Generous, A., Sinn, P.L. & Cattaneo, R. (2015) Connections matter – how viruses use cell–cell adhesion components. *Journal of Cell Science*, 128, 431–439. Available from: https://doi.org/10.1242/jcs.159400

Meier, F., Beck, S., Grassl, N., Lubeck, M., Park, M.A., Raether, O. et al. (2015) Parallel accumulation–serial fragmentation (PASEF): multiplying sequencing speed and sensitivity by synchronized scans in a trapped ion mobility device. *Journal of Proteome Research*, 14, 5378–5387.

Meier, F., Brunner, A.-D., Koch, S., Koch, H., Lubeck, M., Krause, M. et al. (2018) Online parallel accumulation–serial fragmentation (PASEF) with a novel trapped ion mobility mass spectrometer. *Molecular & Cellular Proteomics*, 17, 2534–2545.

Mohanta, T.K., Sharma, N., Arina, P. & Defilippi, P. (2020) Molecular insights into the MAPK cascade during viral infection: potential crosstalk between HCQ and HCQ analogues. *BioMed Research International*, 2020, 8827752.

Mulot, M., Monsion, B., Boissinot, S., Rastegar, M., Meyer, S., Bochet, N. et al. (2018) Transmission of turnip yellows virus by *Myzus persicae* is reduced by feeding aphids on double-stranded RNA targeting the ephrin receptor protein. *Frontiers in Microbiology*, 9, 457. Available from: https://doi.org/10.3389/fmicb.2018.00457

Nasuhidehnavi, A., Zhao, Y., Punetha, A., Hemphill, A., Li, H. & Bechtel, T.J. et al. (2022) A role for Basigin in *Toxoplasma gondii* infection. *Infection & Immunity*, 90(8), e00205-22.

Navas-Castillo, J., Fiallo-Olivé, E. & Sánchez-Campos, S. (2011) Emerging virus diseases transmitted by whiteflies. *Annual Review of Phytopathology*, 49, 219–248. Available from: https://doi.org/10.1146/annurev-phyto-072910-095235

Nesvizhskii, A.I., Keller, A., Kolker, E. & Aebersold, R. (2003) A statistical model for identifying proteins by tandem mass spectrometry. *Analytical Chemistry*, 75, 4646–4658.

Ng, J.C.K. & Perry, K.L. (2004) Transmission of plant viruses by aphid vectors. *Molecular Plant Pathology*, 5, 505–511. Available from: https://doi.org/10.1111/j.1364-3703.2004.00240.x

Ning, W., Jiang, P., Guo, Y., Wang, C., Tan, X., Zhang, W. et al. (2021) GPS-Palm: a deep learning-based graphic presentation system for the prediction of S-palmitoylation sites in proteins. *Briefings in Bioinformatics*, 22, 1836–1847.

O'Leary, N.A., Wright, M.W., Brister, J.R., Ciufo, S., Haddad, D., Mcveigh, R. et al. (2016) Reference sequence (RefSeq) database at NCBI: current status, taxonomic expansion, and functional annotation. *Nucleic Acids Research*, 44, D733–D745.

Okada, A.K., Teranishi, K., Ambroso, M.R., Isas, J.M., Vazquez-Sarandeses, E., Lee, J.-Y. et al. (2021) Lysine acetylation regulates the interaction between proteins and membranes. *Nature Communications*, 12, 6466. Available from: https://doi.org/10.1038/s41467-021-26657-2

Pauchet, Y., Muck, A., Svatoš, A. & Heckel, D.G. (2009) Chromatographic and electrophoretic resolution of proteins and protein complexes from the larval midgut microvilli of *Manduca sexta*. *Insect Biochemistry and Molecular Biology*, 39, 467–474.

Pierleoni, A., Martelli, P.L. & Casadio, R. (2008) PredGPI: a GPI-anchor predictor. *BMC Bioinformatics*, 9, 392.
Polston, J.E. & Anderson, P.K. (1997) The emergence of whitefly-transmitted geminiviruses in tomato in the western hemisphere. *Plant Disease*, 81, 1358–1369. Available from: https://doi.org/10.1094/PDIS.1997.81.12.1358
Popova-Butler, A. & Dean, D.H. (2009) Proteomic analysis of the mosquito *Aedes aegypti* midgut brush border membrane vesicles. *Journal of Insect Physiology*, 55, 264–272.
Qin, F., Liu, W., Wu, N., Zhang, L., Zhang, Z., Zhou, X. et al. (2018) Invasion of midgut epithelial cells by a persistently transmitted virus is mediated by sugar transporter 6 in its insect vector. *PLoS Pathogens*, 14, e1007201.
Savojardo, C., Martelli, P.L., Fariselli, P., Profiti, G. & Casadio, R. (2018) BUSCA: an integrative web server to predict subcellular localization of proteins. *Nucleic Acids Research*, 46, W459–W466.
Sayers, E.W., Bolton, E.E., Brister, J.R., Canese, K., Chan, J., Comeau, D.C. et al. (2021) Database resources of The National Center for Biotechnology Information. *Nucleic Acids Research*, 50, D20–D26. Available from: https://doi.org/10.1093/nar/gkab1112
Sherman, B.T., Hao, M., Qiu, J., Jiao, X., Baseler, M.W., Lane, H.C. et al. (2022) DAVID: a web server for functional enrichment analysis and functional annotation of gene lists (2021 update). *Nucleic Acids Research*, 50, W216–W221.
Stelzer, G., Rosen, N., Plaschkes, I., Zimmerman, S., Twik, M. & Fishilevich, S. et al. (2016) The GeneCards suite: from gene data mining to disease genome sequence analyses. *Current Protocols in Bioinformatics*, 54, 1.30.1–1.30.33.
Szklarczyk, D., Kirsch, R., Koutrouli, M., Nastou, K., Mehryary, F., Hachilif, R. et al. (2023) The STRING database in 2023: protein-protein association networks and functional enrichment analyses for any sequenced genome of interest. *Nucleic Acids Research*, 51, D638–D646. Available from: https://doi.org/10.1093/nar/gkac1000
Tavares, C.S., Mishra, R., Ghobrial, P.N. & Bonning, B.C. (2022) Composition and abundance of midgut surface proteins in the Asian citrus psyllid, *Diaphorina citri*. *Journal of Proteomics*, 261, 104580.
Thurmond, J., Goodman, J.L., Strelets, V.B., Attrill, H., Gramates, L.S., Marygold, S.J. et al. (2019) FlyBase 2.0: the next generation. *Nucleic Acids Research*, 47, D759–D765.
Valero-Rello, A., Baeza-Delgado, C., Andreu-Moreno, I. & Sanjuán, R. (2024) Cellular receptors for mammalian viruses. *PLoS Pathogens*, 20, e1012021. Available from: https://doi.org/10.1371/journal.ppat.1012021
Varma, A. & Malathi, V.G. (2003) Emerging geminivirus problems: a serious threat to crop production. *Annals of Applied Biology*, 142, 145–164. Available from: https://doi.org/10.1111/j.1744-7348.2003.tb00240.x
Villegas-Coronado, D., Guzman-Partida, A.M., Aispuro-Hernandez, E., Vazquez-Moreno, L., Huerta-Ocampo, J.Á., Sarabia-Sainz, J.A. et al. (2022) Characterization and expression of prohibitin during the Mexican bean weevil (*Zabrotes subfasciatus*, Boheman, 1833) larvae development. *Comparative Biochemistry and Physiology Part B: Biochemistry and Molecular Biology*, 262, 110770.
Wang, H., Wu, K., Liu, Y., Wu, Y. & Wang, X. (2015) Integrative proteomics to understand the transmission mechanism of barley yellow dwarf virus-GPV by its insect vector *Rhopalosiphum padi*. *Scientific Reports*, 5, 10971. Available from: https://doi.org/10.1038/srep10971
Watarai, M., Kamata, Y., Kozaki, S. & Sasakawa, C. (1997) rho, a small GTP-Binding protein, is essential for shigella invasion of epithelial cells. *The Journal of Experimental Medicine*, 185, 281–292. Available from: https://doi.org/10.1084/jem.185.2.281
Wickham, H., Averick, M., Bryan, J., Chang, W., McGowan, L., François, R. et al. (2019) Welcome to the Tidyverse. *Journal of Open Source Software*, 4, 1686. Available from: https://doi.org/10.21105/joss.01686
Wolfersberger, M.G. (1993) Preparation and partial characterization of amino acid transporting brush border membrane vesicles from the larval midgut of the gypsy moth (*Lymantria dispar*). *Archives of Insect Biochemistry and Physiology*, 24, 139–147. Available from: https://doi.org/10.1002/arch.940240304
Wu, C., Yang, C., Wang, Y., Wang, J. & Zhu, J. (2023) Molecular characterization and functional analysis of the dipeptidyl peptidase IV from venom of the ectoparasitoid *Scleroderma guani*. *Toxins*, 15, 311. Available from: https://doi.org/10.3390/toxins15050311
Wu, C.H. (2006) The universal protein resource (UniProt): an expanding universe of protein information. *Nucleic Acids Research*, 34, D187–D191.
Yuan, C., Ding, X., Xia, L., Yin, J., Huang, S. & Huang, F. (2011) Proteomic analysis of BBMV in *Helicoverpa armigera* midgut with and without Cry1Ac toxin treatment. *Biocontrol Science and Technology*, 21, 139–151.
Zhang, Y., Wen, Z., Washburn, M.P. & Florens, L. (2010) Refinements to label free proteome quantitation: how to deal with peptides shared by multiple proteins. *Analytical Chemistry*, 82, 2272–2281. Available from: https://doi.org/10.1021/ac9023999
Zhao, J., Chi, Y., Zhang, X.-J., Wang, X.-W. & Liu, S.-S. (2019) Implication of whitefly vesicle associated membrane protein-associated protein B in the transmission of tomato yellow leaf curl virus. *Virology*, 535, 210–217. Available from: https://doi.org/10.1016/j.virol.2019.07.007

Zhao, J., Lei, T., Zhang, X.-J., Yin, T.-Y., Wang, X.-W. & Liu, S.-S. (2020) A vector whitefly endocytic receptor facilitates the entry of begomoviruses into its midgut cells via binding to virion capsid proteins. *PLoS Pathogens*, 16, e1009053. Available from: https://doi.org/10.1371/journal.ppat.1009053

Zybailov, B., Mosley, A.L., Sardiu, M.E., Coleman, M.K., Florens, L. & Washburn, M.P. (2006) Statistical analysis of membrane proteome expression changes in *Saccharomyces cerevisiae*. *Journal of Proteome Research*, 5, 2339–2347. Available from: https://doi.org/10.1021/pr060161n

SUPPORTING INFORMATION

Additional supporting information can be found online in the Supporting Information section at the end of this article.

How to cite this article: Jiménez, J., Mishra, R., Wang, X., Magee, C. M. & Bonning, B. C. (2024) Composition and abundance of midgut plasma membrane proteins in two major hemipteran vectors of plant viruses, *Bemisia tabaci* and *Myzus persicae*. *Archives of Insect Biochemistry and Physiology*, 116, e22133. https://doi.org/10.1002/arch.22133